Proc. XIX Iberoamerican Symp. on Catalysis, Merida, Mexico, 2004, 3437-3446

Copper Mordenite as a de-NO_x Catalyst: Role of Variable Silica-Alumina Ratio and Effects of Adsorbed Water

A. Efimov[a], V. Petranovskii*[,b], R. Marzke[c], A. Pestryakov[d,e], M.-Á. Hernández Espinosa[f], F. Chávez-Rivas[g]

[a] St. Petersburg State University, Chemistry Department, St. Petersburg, 198504, Russia
[b] Centro de Ciencias de la Materia Condensada, UNAM, Ensenada 22800, México; * vitalii@ccmc.unam.mx
[c] Physics and Astronomy Department, Arizona State University, Tempe, AZ 85287, USA
[d] Tomsk State University of Civil Engineering, Solanaya sq., 2, Tomsk 634003, Russia
[e] Fritz Haber Institute, Faradayweg 4-6, D-14195 Berlin, Germany
[f] Instituto de Ciencias, Universidad de Puebla, Puebla, México
[g] Área de Química Aplicada, UAM-A, Av. San Pablo 180, 02200 México

Resumen

Presentamos medidas en las Cu-mordenitas que demuestran que la relación molar sílice-alumina (RM) de mordenitas afecta fuertemente la eficacia de la conversión para NO_x, y que estos catalizadores están entre los más activos para el *de*-NO_x en las temperaturas moderadas. La desactivación rápida de Cu-mordenitas por el agua nos ha conducido también a investigar los efectos del agua adsorbida en los iones estructurales y extra-estructurales, usando RMN de ^{27}Al y ^{1}H. El contenido de agua adsorbida ha sido controlado en muestras de mordenita vía análisis termogravimetrico (TGA), así como por la calcinación en vacío. Varias medidas de RMN de protón se han realizado para la interpretación de espectros, incluyendo variable "pulse-delay spin echo" y $^{1}H/\ ^{27}Al$ TRAPDOR. Varias técnicas de caracterización superficial se han aplicado a las mordenitas protonadas e intercambiadas con Cu.

Palabras clave: mordenita; relación molar SiO_2/Al_2O_3; *de*-NO_x; desactivación;

Abstract

We report measurements in copper mordenites showing that silica-alumina molar ratio (MR) strongly affects conversion efficiency for NO_x, and that these catalysts are among the most active available for *de*-NO_x at moderate temperatures. Copper mordenites' rapid deactivation by water has led us to also investigate the effects of adsorbed water on framework and extra-framework ions, mainly using NMR of ^{27}Al and ^{1}H. Adsorbed water content has been monitored and controlled in mordenite samples via TGA, as well as by vacuum calcination. Several proton NMR measurements have been performed to aid in the interpretation of spectra, including variable pulse-delay spin echo and $^{1}H/\ ^{27}Al$ TRAPDOR. A number of surface characterization techniques have been applied to both H and Cu mordenites.

Key words: mordenite; SiO_2/Al_2O_3 molar ratio; *de*-NO_x; deactivation;

Introduction

The diversity of natural and synthetic zeolites [1,2] constitutes an inexhaustible field for research on the synthesis of nanomaterials with controlled chemical, catalytic, optical, and magnetic properties [3,4]. In contrast with amorphous matrices like nanostructured titania, alumina, silica, etc., the crystallinity of zeolites *a priori* furnishes a special organization to the system, although this organization can be very complicated due to the complexity of real zeolite crystal lattices. Unlike some matrices that are simpler in chemical composition, zeolites appear not only as a supporting surface for geometrical and topological reasons, but also as an active ionic medium promoting a rich chemistry of metal ions incorporated with reactants like water, alkali ions or different acidic centers [1]. Transition metal ions within such nanoporous media as zeolites are efficient modifiers of their properties. Through them, zeolite matrices combine the factors of nanoporosity and nanome-

Preprint of the Department of Inorganic Chemistry, Fritz-Haber-Institute of the MPG *(for personal use only)* (www.fhi-berlin.mpg.de/ac)

ter-scale chemical reactivity on a broad scale, with respect to other ions. Zeolite hosts thus have significant practical importance as catalyst supports, and the state of copper is of interest from the point of view of catalytic activity management [5-7].

Control of copper incorporation for production of Cu-zeolite catalysts (e.g., for selective catalytic reduction of NO_x [3,5]) has been extensively studied to date, but no unambiguous general rules associating the catalytic activity and chemical composition of similar catalysts are known. The reason for this is a wide difference in Cu adsorption sites in zeolites for Cu^+ and Cu^{2+} ions [8,9]. Cu^+-ions in zeolites are fairly stable, whereas the Cu^{2+}-ions supported on other amorphous or crystalline matrices without explicit ionic properties are reducible to Cu(0) much easier. This might be one reason for the higher efficiency of a zeolite framework structure with active ionic properties in catalysis, while other supports are much worse for the selective catalytic reduction of NO_x [5,10].

It is reasonable to expect that changing the chemical composition of the mordenite framework leads to major changes in the occupation of sites by individual non-framework atoms. The framework of mordenite possesses several positions for copper localization, and there are noticeable changes in water tolerance and hydrothermal stability under heating, dehydration, reduction, etc. [11-13]. Analysis by a Monte Carlo procedure has shown that pairs of closely-spaced Brønsted acid (H^+) sites, which are one means of binding extra-framework Cu^{2+} cations, are distributed with a probability that is highly sensitive to MR [12]. Thus in NO reduction under lean NO_x wet conditions [11], it is not surprising that MR is one of the crucial characteristics determining Cu zeolites' overall effectiveness and lifetime for NO conversion. This has led us to investigate the effects of adsorbed water on framework and extra-framework ions, mainly using MAS NMR of ^{27}Al and ^{1}H. We have also correlated our findings with results of direct measurements of the catalytic properties of Cu-mordenites, e.g. NO conversion rates.

Experimental

Samples were prepared from H^+ mordenites with MR values from 10 to 206, furnished originally via the TOSOH Corporation of Japan [1]. Cu^{2+} exchange was performed with 0.1 molar aqueous copper nitrate solutions. The samples were dried, and several were treated by reduction in flowing H_2 for 4 h at 350 °C. Copper content was monitored by atomic absorption spectrometry. Catalytic activity was measured in a continuous flow reactor, and solid state magic angle spinning (MAS) NMR spectra were recorded on a Varian CMX Infinity solids NMR spectrometer operating at 300 MHz for protons. Diffuse reflectance optical spectra were recorded on a Varian Cary 300 spectrophotometer, and EPR spectra were recorded at JOEL JERRES3X spectrometer at 8.86 GHz using power 1 mW and modulation frequency of magnetic field of 100 KHz. Surface area S_{BET} and micropore volume V_Σ were determined by high-resolution nitrogen adsorption measurements on an Autosorb-1 Quantachrome equipment in the range of $10^{-6} < p/p_o < 1$. The crystal structure of the initial mordenite samples was determined by X-ray diffraction (XRD) measurements on a Philips diffractometer, model X'Pert, equipped with a curved graphite monochromator, using Cu K_α radiation. TPD measurements were done on a Bell Japan, Inc. TPD-1-AT apparatus, using standard procedures. Brønsted acidity of the surface was measured by potentiometric titration.

Results and discussion

An extensive set of mordenites, including highly dealuminated up to MR=206, was used in this study. Making an assumption that crystal structure could be significantly influenced during dealumination, crystallinity of the samples was tested. There are no significant differences in the values of *"a", "b"* and *"c"* for the entire series of HMor samples. Detailed discussion and refinement of crystalline structure of this mordenite series is beyond the scope of the present work and will be given elsewhere. The most important conclusion for this paper is that sample crystallinity is not affected by the dealumination treatment and neither degradation of crystalline pattern nor appearance of amorphous phases is observed.

The results of HMor porosity characterization and copper content measurements are presented in Table 1. The S_{BET} value increases with MR growth; a maximum increment occurs in going from HMor15 to HMor30. Meanwhile, the total pore volume V_Σ goes through a minimum for HMor15. It is important to note that in the case of ideal mordenite crystals possessing regular channels with elliptical cross-section 0.65×0.70 nm, the material has a micropore volume equal to 0.14 cm^3/g [1]. Higher values of the observed micropore volume than that of the perfect mordenite crystal, as well as mesopore volume (with non-structural radii up to 50 nm), are thus associated with defects in the microcrystals, probably originating from the original TOSOH synthesis. These defects provide an additional contribution to V_Z, due to irregular porosity inside the crystal volume.

The variation of total observed surface area shows that the microstructure of these matrices depends on MR, although the crystal structure shows only a subtle variation with MR. Some correlation in the data on the total surface area and pore volumes exists, and the least "porous" HMor15 is characterized by the lowest values of mesopore volume. The mesopores can be associated with cleaved areas of microcrystals, defects, uneven surface, etc., and they seem to be nearly independent of the amount of Si substituted by Al in ideal tetrahedral TO_4 coordination. Meanwhile, according to these data HMor15 has the minimum concentration of defects and other above-mentioned structural features that lead to porosity increase. Thus, HMor15

Table 1. Characteristics of mordenites used.

	HMor10	***HMor15***	HMor30	**HMor206**
S_{BET}, m^2/g	359	380	480	493
S_t, (external surface) m^2/g	45	33	51	68
V_Σ, cm^3/g	0.200	0.174	0.238	0.261
Mesopore volume, cm^3/g (Pore radii 2-50 nm)	0.07	0.05	0.06	0.05
Al concentration derived from MR, mol/kg	2.56	1.83	1.01	0.16
TPD-derived conc. of acid sites, mol/kg	0.44	1.24	0.49	0.13
Copper content after ion exchange, wt %	0.79	0.26	0.26	0.44
Maximum (theoretical) ion-exchange capacity on the basis of MR, with respect to Cu^{2+}, wt % of Cu	8.2	5.9	3.2	0.5
% of ion exchange	9.6	4.4	8.1	86.3

is expected to have the most perfect crystal structure within the given series. That may be a reason for the especially favorable behavior of copper ions in this mordenite.

Isotherms of N_2 adsorption at 76 K (Figure 1) confirm these conclusions also. The sample HMor15, unlike the other mordenites, exhibits a saturation zone in the interval of $0.1 < p/p_0 < 0.8$, indicating that the micropores are homogeneous, and only a mild increase in the capacity of adsorption for $p/p_0 > 0.9$ is observed. For the samples HMor30 and HMor206 hysteresis cycles are better defined, and for HMor10 they are pronounced, indicating a higher contribution of mesopores in these samples.

Complete exchange of 2 H^+ ions in HMor for Cu^{2+} ion leads to the composition $Cu^{2+}{}_xAl_{2x}Si_yO_{96}$, where y/x=MR; the amount of copper is expected to change with changing MR. Copper content was measured for ion exchanged samples, and the degree of the ion-exchange was calculated (Table 1). Experimental results demonstrate that all the samples do not attain the complete exchange. That is, only small part of the acid sites is active in the copper incorporation. For example, less than 10% of the total occupancy is attained for HMor10, HMor15, and HMor30. It is expected that Cu^{2+}-ions will occupy the more energetically favorable centers in these mordenites. This observation is confirmed by EPR spectra (Figure 2). They demonstrate only one specific site for Cu-ions for MR 10, 15 and 30, the line with g=2.05 of paramagnetic Cu^{2+} with hyperfine interaction, in extra-framework positions. Small line with g=4.3 can be due to Fe^{3+} impurity or due to Cu^{2+} that enter in some defects of zeolite structure in tetrahedral framework positions.

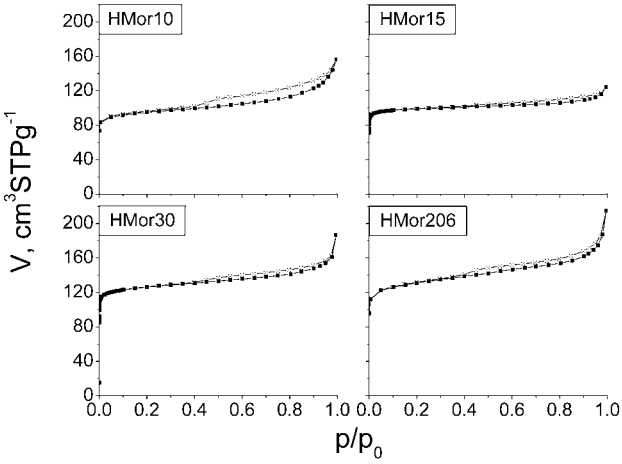

Figure 1. Isotherms of N_2 adsorption of the HMor set.

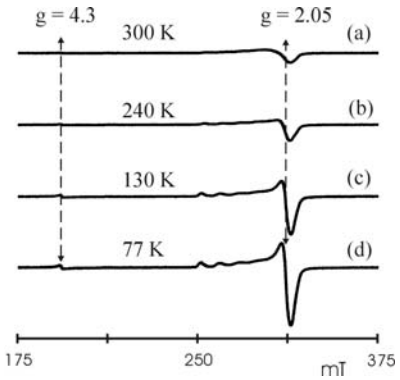

Figure 2. EPR spectra of Cu-Mordenite with MR=10

There are at least three main maxima at the ammonia TPD curves, the relative contribution of which varies with MR. The lowest-temperature peak, ca. 490 K, which dominates for HMor10 sample, belongs to weakly bonded ammonia adsorbed probably on extra-framework Lewis sites. Intensity of this peak decreases with increasing MR. The TPD curve for HMor10 also has a shoulder, from which a maximum at ca. 660 K can be resolved. A pronounced maximum at ca. 730 K occurs for the other three mordenites, with little shift to lower temperatures from HMor15 to HMor206. These maxima are not symmetrical, and contributions from several species that develop peaks at 660 K can be evaluated. The above three ammonia TPD peaks, 450-490 (very likely Lewis), 660 and 730 K (Brønsted), are associated with the three different groups of acid sites, the amount of which is very variable for different MR.

Since ammonia TPD results are characteristic of the whole set of the acid centers in a sample, it was of interest to detect individual acid sites with different strength. The surface concentration of non-equivalent Brønsted acid sites (BAS) with different pK_a was determined by non-aqueous titration. The results are listed in Table 2. All samples have a number of distinct types of BAS in wide range of pK_a. HMor10 sample has four types of BAS with weak and moderate strength ($2.8<pK_a<5.7$), which correlate with the above TPD data. A large quantity of strong BAS ($1.5<pK_a<2.3$) is present in HMor15, although some sites

Table 2. Specific concentration and pK_a of Brønsted acid sites for the set of mordenites

HMor10		HMor15		HMor30		HMor206	
BAS pK_a	C_{BAS}, μmol/m^2	BAS pK_a	C_{BAS}, μmol/m^2	BAS pK_a	C_{BAS}, μmol/m^2	BAS pK_a	C_{BAS}, μmol/m^2
		1.5	0.92			1.5	0.32
		2.0	1.00	1.8	0.50	1.8	0.34
2.8	0.18	2.3	0.76	2.9	0.92	2.4	0.36
3.9	0.22			3.4	0.52	3.3	0.24
5.0	0.84	5.5	0.18	5.0	0.20	4.0	0.06
5.7	0.24	6.1	0.28	5.6	0.10	5.4	0.06

with weak and medium strength ($5.5<pK_a<6.1$) are present on its surface in small amounts. It is worth noting that HMor15 has also the weakest acid sites with $pK_a=6.1$, in line with the high concentration of the BAS with the most acid properties ($pK_a=1.5$). The same BAS with $pK_a=1.5$ are present at HMor206 in relatively high concentration, while only very low amounts of other types of BAS with $pK_a>3.3$ exist on the surface of this sample.

Catalytic activity for NO_x attained conversion levels in excess of 90% for H-reduced samples of Cu mordenite with intermediate MRs from 15 through 30. Light-off temperatures were approximately 300 °C. Cu mordenite 10 and 206 were markedly less efficient, over most of the temperature range studied (180 – 600 °C) (Figure 3).

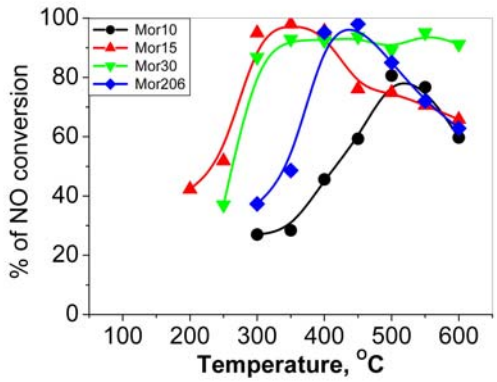

Figure 3. Data on NO conversion in SCR reaction with propane.

Water and Al in H-mordenite 15 and H-mordenite 20: Al and proton NMR, with proton T2 spectral editing and TRAPDOR monitoring of Al H proximity

The large amount of water present in zeolites under ambient conditions is indicated by their standard chemical compositions, for example Na-mordenite's formula $Na_8(H_2O)_{24}$: $Si_{40}Al_8O_{96}$ at silica-alumina ratio 10 [1]. In this structure one water molecule is entrained for every two Si atom sites, and there are three times as many waters as Al atoms. Such a large affinity of zeolites for water raises the questions of where and how the molecules are incorporated into the structure, and during the 1980s Luz and Vega conducted an extensive multi-nuclear NMR investigation aimed at answering these questions, mainly in the zeolite H-rho [14]. They obtained spectra of all three of the most important zeolite nuclei – ^{27}Al, ^{29}Si and ^{1}H – in the presence of controlled amounts of water and methanol, and they also studied ^{2}H, adding D_2O and perdeuterated methanol to samples. Our work to date has been directed towards a different family of zeolites, mordenites, which can have widely varying silica-alumina ratios, but we have asked the similar questions while employing some different approaches. First, ^{27}Al spectra have been obtained from dehydrated and partially rehydrated H-mordenite 15 and Cu-mordenite 15. As shown in Figure 4, these clearly show the dramatic changes in Al environment caused by water removal in both zeolites. However we have concentrated mainly on proton NMR, using the method of two-pulse spin echoes with variable delay times to obtain T_2-weighted proton spectra of partially rehydrated H-mordenite 15 and 20 (Figure 5). Signals from proton species with short T_2 values rapidly disappear from these spectra as the interpulse delay time is increased, leading to patterns for ^{1}H spectra of a zeolite that may differ considerably from those seen in the literature [15,16]. We have also combined such T_2-based spectral editing with a series of NMR measurements that detect proximity of a proton-containing group to Al, an approach known as dipolar dephasing, or TRAPDOR [17-19]. Identification of several main lines in the proton spectra of the two zeolites studied has been facilitated, as discussed below.

As in our previous NMR studies [20], all measurements were taken on H- or Cu-mordenites obtained from or prepared from materials furnished by the TOSOH Corporation of Japan. An earlier proton NMR study was conducted by Baba et al. on H-mordenites from TOSOH [21], with fully dehydrated samples and with a radio frequency pulse sequence that gave spectra strongly resembling some we have taken at short interpulse delay times. Baba et al. identify two proton lines in dehydrated H-mordenite 19 and 106 samples at 1.8 and 4.2 ppm (with respect to TMS), as belonging to silanol groups and acidic OH groups in mordenite. In our studies the zeolite surfaces were treated in two different ways, one to remove water by mild heating to 200 ^{O}C with pumping to 10^{-6} torr, the other to measure the surface water content by TGA. Proton and ^{27}Al spectra were taken of samples before and after these treatments. TGA results for H-mordenite 15 showed a

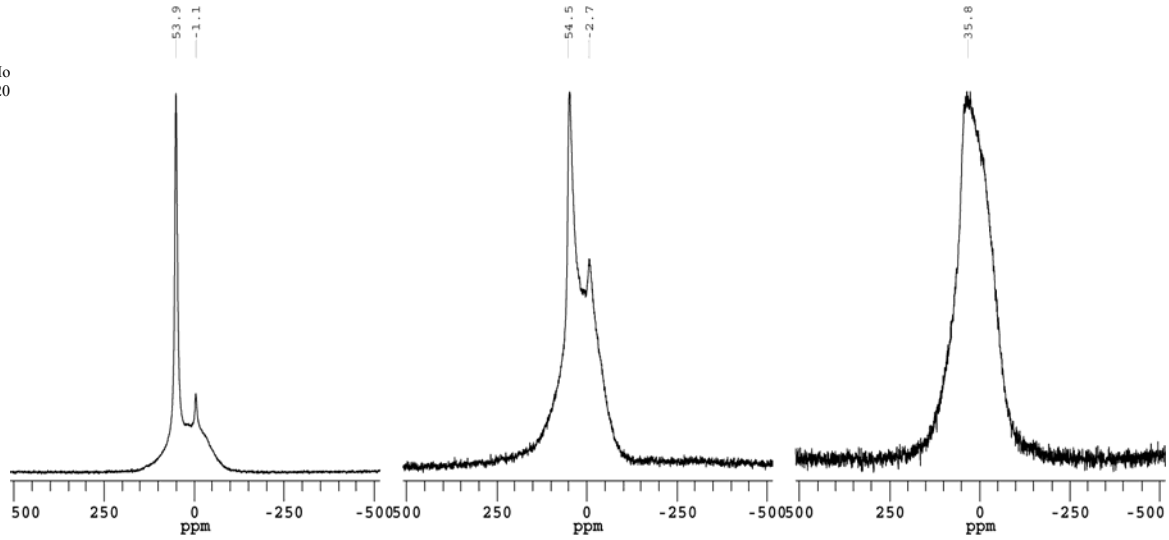

Figure 4. ^{27}Al NMR spectra of a sample of copper mordenite 15 at different stages of dehydration. Conditions: 16,384 acquisitions, room temperature, tip angle < 15°. Left: sample at ambient, showing 4 and 6-fold Al coordination lines near 54 and 0 ppm, respectively. Center: sample dehydrated, then rehydrated by exposure to air for approximately one hour. Right: a sample fully dehydrated by heating in He, for TGA, to 400 ^{O}C. This last treatment produced Al line intensity in the vicinity of 5-fold coordinated Al species, a result not yet understood. Strong overall decrease in signal intensity left-to-right is indicated by the increase in the noise level of the spectra.

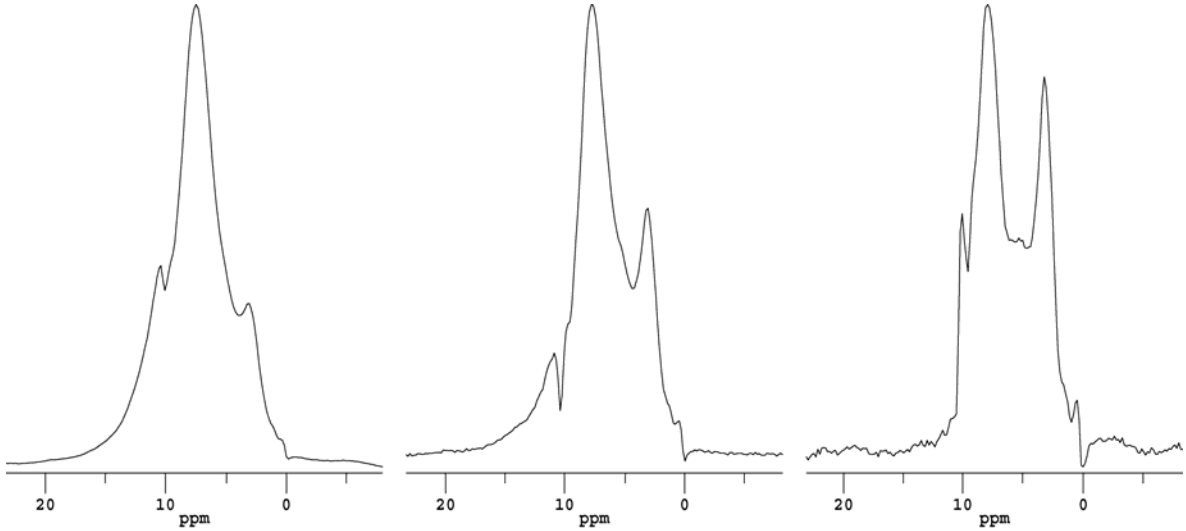

Figure 5. Proton NMR line shapes acquired in partially dehydrated H mordenite 20, using a standard 2-pulse spin echo sequence with variable delay time between 90° and 180° pulses.
Left: delay 200 μs. Center: delay 400 μs. Right: delay 600 μs.

fractional water weight loss close to 10%, significantly less than that found by Bogdanchikova et al. for the same zeolite [22].

Like Baba et al., we observe a sharp line at the silanol position, but in partially rehydrated samples of both H-mordenite 15 and 20 a line arising from water (6.2 ppm) is prominent (Figure 6). There is in H-mordenite 20 a weak line near 4 ppm and another line, water-associated, appears at 8.4 ppm. The 6.2 ppm water line in both mordenites is close to an intermediate water-content line seen by Luz and Vega in their proton spectra of water-treated H-rho zeolite. At high water content in our samples the single, large line we observe is at 5.4 ppm, similar to the 4.6 ppm line seen by Luz and Vega.

The existence of a line close to 4 ppm, barely distinguishable in the spectrum of H-mordenite 20, turns out to be required in order to deconvolve all of our observed spectra for both mordenites into a set of distinct lines, following standard practice in NMR. However this 4 ppm "line" is quite broad (~ 2 kHz) and it is appears almost as background, behind the sharper lines from water and SiOH. As shown in Figure 7 below, however, the results of preliminary TRAPDOR experiments in H-mordenite 20 to detect proximity of protons to Al are best interpreted as affecting mainly this broad line, leaving the narrower ones relatively unchanged. Based in part on the proton NMR studies of Freude at al. on H-ZSM-5 and H-Y zeolites [16,17], we infer that the broad background line contains strong contri-

butions from acid sites in the zeolite, both types of which (Brønsted or Lewis) have proton sites neighbouring directly on an Al ion [22,23]. At this time we cannot distinguish whether the line contains contributions from one or the other kind of acid site. Its breadth can even be due to the presence of several species, since water's association with Lewis sites is possible [16], but the line's position is close to that generally associated with Brønsted sites. In either case, however, the association with Al appears to be confirmed by the TRAPDOR data.

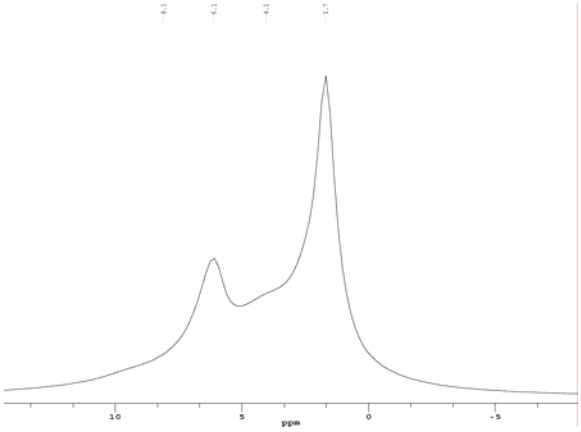

Figure 6. The proton spectrum of partially dehydrated H-mordenite 20, obtained with a spin echo delay time of 100 μs. Note weak lines near 4 and 8 ppm.

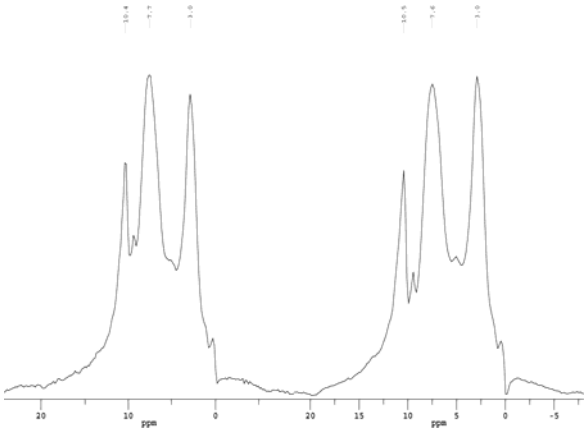

Figure 7. The TRAPDOR effect upon the proton spectrum of partially dehydrated H-mordenite 20, at pulse delay 500 μs. Left: normal spectrum without irradiation at the ^{27}Al frequency. Right: the spectrum after ^{27}Al irradiation, showing a reduction in the level of overall signal in the range 5 - 10 ppm.

Our principal findings to date are thus as follows. As in other zeolites, for H-mordenite 15 and Cu-mordenite 15 the effect of dehydration by either surface treatment is to strongly broaden, almost to the point of disappearance, the NMR spectra of ^{27}Al. In partially rehydrated H-mordenite 15 and 20, two distinguishable lines from the T_2-weighted spin echo spectra are identified with SiOH at 1.7 ppm and water at 6.2 ppm. Clearly visible in the longer interpulse delay TRAPDOR spectra for rehydrated H-mordenite 20 is a narrow line at ~8.4 ppm, which is not seen in the spectrum of the fully dehydrated material. In addition to these is a broad line (or group of lines) close to 4 ppm, weakly visible in the spectrum of partially rehydrated H-mordenite 20, but contributing mostly to a background of signal intensity in H-mordenite 15. In rehydrated H-mordenite 20 this line exhibits a weak dipolar dephasing or TRAPDOR effect, decreasing significantly in size when the sample is subjected to strong pulsed irradiation at the ^{27}Al NMR frequency. The line is therefore identified with the proton or protons associated with acid sites, in both mordenites. Its apparent weakness in our H-mordenite 20 TRAPDOR sample may be partly due to the substantial amount of water reabsorbed by this sample, before measurements were taken.

Conclusions

The set of mordenites with MR in the range from 10 through 206 demonstrate clear dependence of all properties under study on chemical composition of zeolite matrix. Within the series of mordenite samples MR serves as a key factor for regulation of both concentration and strength of the acid centres. Altogether, hydrogen-reduced Cu-mordenites with intermediate MRs 15 – 30 are highly effective for *de*-NO_x catalysis. Standard proton NMR spectra of H and Cu mordenite showed patterns similar to those of ZSM-5, but spin echo spectra showed strong changes at increasing pulse delays, allowing some application of T_2-based spectral editing. TRAPDOR indicated the proximity to Al of the protons under observation. Water adsorption-desorption effects upon ^{27}Al spectra are substantial, especially for Cu mordenite, and show that Al strongly coordinates with H_2O. The strong affinity of water for Al in mordenite structures is evident from the NMR spectra of both H and Al.

Acknowledgements

We have benefited greatly from many discussions and collaborations with Drs. Yoshihiro Sugi and Naonobu Katada. Thanks are given to Jose Victor Tamariz Flores for his investigations of Cu content, to Inocente Rodriguez-Iznaga, Dimitry Kovalenko, Pornsawan Kanchanawanichkun and Araya Kittivanichawat for their experimental work and to Israel Gradilla, Eloisa Aparicio, Juan Peralta and Eric Flores for valuable technical support. This research was supported by CONACYT, Mexico through grant # 32118-E, UNAM-PAPIIT through grant IN114603-3 and by the Mexico-U.S. Materials Corridor Partnership Initiative, DOE #DE-FC04-01AL67097.

References

1. D.W. Breck, Zeolite Molecular Sieves. Structure, Chemistry and Use, A Wiley-Interscience Publication, John Wiley & Sons: New York, 1974.
2. Atlas of Zeolite Structure Types, 5th revised edition, (Ch. Baerlocher, W.M. Meier, D.H. Olson, Eds.), 2000.
3. V.I. Parvulescu, P. Grange, B. Delmon, Catal. Today 46 (1998) 233.
4. Ph. Moriarty, Rep. Progr. Phys. 64 (2001) 297.
5. P. Gilot, M. Guyon, B.R. Stanmore, Fuel 76 (1997) 507.
6. C. Torre-Abreu, C. Henriques, F.R. Ribeiro, G. Delahay, M.F. Ribeiro, Cat. Today 54 (1999) 407.
7. Z. Chajar, V. Le Chanu, M. Primet, H. Praliaud, Catal. Lett. 52 (1998) 97.
8. M.W. Anderson, L. Kevan, J. Chem. Soc.-Faraday Trans. I 83 (1987) 3505.
9. M.W. Anderson, L. Kevan, J. Phys. Chem. 91 (1987) 4174.
10. M. Guyon, V. Le Chanu, P. Gilot, H. Kessler, G. Prado, Stud. Surf. Sci. Cat. 116 (1998) 297.
11. S.Y. Chung, S.H. Oh, M.H. Kim, I.S. Nam, Y.G. Kim, Cat. Today 54 (1999) 521.
12. B.R. Goodman, K.C. Hass, W.F. Schneider, J.B. Adams, Cat. Lett. 68 (2000) 85.
13. M.P. Attfield, S.J. Weigel, A.K. Cheetham, J. Catal. 170 (1997) 227.
14. Luz Z., Vega A.J, J. Phys. Chem. 91 (1987), 374-382.
15. J.L. White, L.W. Beck, J.F. Haw, J. Am. Chem. Soc. 114 (1992) 6182.
16. I. Wolf, D. Freude, Microporous Materials 5 (1995) 69.
17. D. Freude, Chem. Phys. Lett. 235 (1995) 69.
18. L.W. Beck, J.L. White, J.F. Haw, J. Am. Chem. Soc. 116 (1994) 9657.
19. C.P. Grey, A.J. Vega, J. Am. Chem. Soc. 117 (1995) 8232.
20. V. Petranovskii, R. Marzke, G. Diaz, A. Gomez, N. Bogdacikova, S. Fuentes, N. Katada, A. Pestryakov, V. Gurin, Stud. Surf. Sci. Catal. 142 (2002) 815.
21. T. Baba, N. Komatsu, Y. Ono, H. Sugisawa, T. Takahashi, Micropor. Mesopor. Mater. 22 (1998) 203.
22. N. Bogdanchikova, V. Petranovskii, S. Fuentes, E. Paukshtis, Y. Sugi, A. Licea-Claverie, Mater. Sci. Eng. A 276 (2000) 236.
23. M. Hunger, D. Freude, D. Fenzke, H. Pfeifer, Chem. Phys. Lett. 191 (1992) 391.

Preprint of the Department of Inorganic Chemistry, Fritz-Haber-Institute of the MPG *(for personal use only)* (www.fhi-berlin.mpg.de/ac)